

## Article

# Chaos Regulation via Complex Nonlinear Feedback and Its Implementation Based on FPAA

Jitong Xu <sup>1</sup>, Chunbiao Li <sup>2,3,\*</sup>, Xiaoliang Cen <sup>2</sup>, Xin Zhang <sup>2</sup> and Lin Chai <sup>4</sup>

<sup>1</sup> School of Integrated Circuits, Nanjing University of Information Science & Technology, Nanjing 210044, China; jitongxu@nuist.edu.cn

<sup>2</sup> School of Electronics and Information Engineering, Nanjing University of Information Science & Technology, Nanjing 210044, China; xiaoliangcen@nuist.edu.cn (X.C.); xinzhang96@nuist.edu.cn (X.Z.)

<sup>3</sup> School of Artificial Intelligence, Nanjing University of Information Science & Technology, Nanjing 210044, China

<sup>4</sup> Jinan Key Laboratory of Memristive Computing and Applications (JKLMCA), Qilu Institute of Technology, Jinan 250200, China; chailin@qlit.edu.cn

\* Correspondence: goontry@126.com or chunbiaolee@nuist.edu.cn; Tel.: +86-139-1299-3098

**Abstract:** Complex nonlinear feedback is a key factor in the generation of chaos. In many cases, complex nonlinear functions have a higher probability for chaos producing, and correspondingly new bifurcations may be triggered in the dynamical system. Due to the difficulty in circuit implementation of complex nonlinear feedback, researchers often introduce simple nonlinear constraints to study the occurrence and evolution of chaos. In fact, the impact of complex nonlinear feedback on chaotic dynamics deserves further investigation. In this work, complex nonlinear feedback is introduced into an offset-boostable chaotic system as an example to observe and analyze its regulatory effect on the dynamics. Complex nonlinear feedback may destroy the property of symmetry of a system; therefore, we examine the evolution of chaotic attractors under the corresponding feedback and the functional transformation between bifurcation and non-bifurcation parameters as well. By fully utilizing the flexible configuration advantages of Field Programmable Analog Array (FPAA), arbitrary complex nonlinear functions are implemented to verify the chaotic dynamics.

Academic Editor: Antonio Palacios

Received: 13 January 2025

Revised: 24 January 2025

Accepted: 28 January 2025

Published: 31 January 2025

**Citation:** Xu, J.; Li, C.; Cen, X.; Zhang, X.; Chai, L. Chaos Regulation via Complex Nonlinear Feedback and Its Implementation Based on FPAA. *Symmetry* **2025**, *17*, 212. <https://doi.org/10.3390/sym17020212>

**Copyright:** © 2025 by the author. Licensee MDPI, Basel, Switzerland. This article is an open access article distributed under the terms and conditions of the Creative Commons Attribution (CC BY) license (<https://creativecommons.org/licenses/by/4.0/>).

**Keywords:** chaos; complex nonlinear feedback; non-bifurcation parameter; Field Programmable Analog Array (FPAA)

## 1. Introduction

Chaos, as a complex nonlinear phenomenon, exhibits unpredictable butterfly effects due to different initial conditions and tiny perturbations. Chaos exists widely in nature, such as in atmospheric systems, ecosystems, mechanical systems, chemical systems, and even financial systems. The widespread chaotic dynamics require careful observation and analysis, as well as effective regulation. At the same time, the random and broadband properties of chaotic signals play an important role in engineering fields such as image encryption [1–3], neuroscience [4–7], and chaos radar [8,9]. The realization of chaos regulation [10] facilitates the application of chaos. In circuit systems, chaotic oscillations are generated by selecting and regulating feedback loops through the collaboration of nonlinear circuit components, such as the triode, with other dynamic components, like inductors and capacitors [11]. As we can imagine, the non-linear relationship hidden in the

voltage and current constraints within a triode is complex, especially at high frequencies. It is very necessary to study complex nonlinear feedback in an actual system.

For specific chaotic systems, the introduction of negative feedback can make the system more stable and reduce the impact of external disturbances on system behavior [12], while the positive feedback typically drives the system to divergence, causing it to break away from equilibrium [13]. The combination of positive and negative nonlinear feedback in a system generates complexity and deterministic chaos [14]. Compared to linear feedback, nonlinear feedback is more common in nature. Linear feedback is often used to control system stability or reduce error, where the response of the system is more linear to the input and easy to predict. Nonlinear feedback, on the other hand, typically leads to more complex dynamics, such as chaos or other undesired oscillations, where the response of the feedback is normally nonlinear and, correspondingly, more difficult to predict. Nonlinear feedback makes the system exhibit more complex dynamics and show noise-like evolution. From the thermodynamic perspective, the evolution of the physical world is a process of entropy increasing, and the underlying foundation is the widespread presence of nonlinear feedback.

Regarding the study of chaos [15], one usually introduces some simple nonlinear feedback [16], such as squared terms [17,18], cubic terms [19,20], or absolute value terms [21,22], to induce chaos and observe its evolution. However, the feedback from relatively complex nonlinear feedback functions, such as trigonometric functions, inverse trigonometric functions, exponential functions, and their complex combinations, is often ignored. On the one hand, this feedback tends to introduce more complex dynamics to the system; on the other hand, these complex nonlinear feedback functions are difficult to implement using conventional circuit components. With the development of electronic technology, especially integrated circuits and programmable devices, there are more options for the circuit implementation of chaotic systems, including analog circuits, digital systems based on microcontrollers [23], Field Programmable Gate Arrays (FPGAs) [24], and Field Programmable Analog Arrays (FPAs) [25]. FPAs integrate various basic units required for analog circuits into chip-like building blocks, and the connections between units are set by programming software AnadigmDesiger2(version 2.8.0.10). Their high-speed operational amplifiers and surrounding resistor-capacitor circuits, input units, output units, clock circuits, reference voltages, and lookup tables endow FPAs with greater integration and adaptability. Based on the platform of an FPA, it is convenient to develop and implement various analog circuits, including chaotic oscillators, and to quickly maintain and upgrade the corresponding application systems. An FPA can serve as an intermediate medium and low-risk transition path for analog ASIC development. The voltage transfer function inside an FPA can approximate various complex nonlinear functions within a certain voltage range, thus providing a new implementation channel and research method for the realization of chaotic circuits.

In fact, complex nonlinear feedback does not indicate that its implementation methods and circuits are necessarily complex. Some individual devices in nature often show complex electromagnetic constraints, and the connections of these devices sometimes effectively modify the chaotic output of the system to meet engineering requirements. In this work, the influence of complex nonlinear feedback on chaotic dynamical systems is further analyzed, including its influence on bifurcation parameters and non-bifurcation parameters. Complex nonlinear feedback will typically revise the original bifurcation behavior of the system, altering its bifurcation path, and may also cause the original non-bifurcation parameters to lose efficacy triggering undesired new bifurcations. The impact and regulation of this complex nonlinear feedback on the system dynamics are ultimately verified on the platform of an FPA circuit. In this work, an offset-boostable chaotic system, VB5, is selected, which has one independent offset parameter. Complex nonlinear

functions are introduced to deeply observe the impact of nonlinear feedback on chaotic dynamics. Based on FPAA, the oscillations of the corresponding chaotic system are further verified and observed. By introducing complex nonlinear feedback into the chaotic system VB5, this work can help to find and design, or even control, chaos in nonlinear systems associated with various engineering applications. The paper is organized as follows: in Section 2, the impact of complex nonlinear feedback on two types of non-bifurcation parameters in the VB5 system is analyzed and the impact of nonlinear feedback on dynamical regulation is observed; Section 3 verifies the oscillations of the corresponding versions of chaotic systems based on the FPAA platform; and a summary and conclusions are given in Section 4.

## 2. Dynamics of Chaotic Systems with Complex Nonlinear Feedback

### 2.1. Complex Nonlinear Electromagnetic Constraint Relation in Nature

There are many nonlinear constraint relationships in nature. In the field of electronics and electrical engineering, diodes, transistors, and field-effect transistors operate in different working regions under different biases. The capacitance property of the PN junction in varactor diodes also changes nonlinearly with the offset voltage. Ferromagnetic materials, due to their high magnetic permeability and nonlinear hysteresis effects, exhibit special nonlinear characteristics. Meanwhile, some dielectric materials, such as thin layers of alumina, may exhibit nonlinear electron tunneling effects. With the development of artificial intelligence and the deepening of research on in-memory computing, the preparation and application of memristors [26] are increasingly valued. The electromagnetic constraint relationship of memristors is more complex, and the resistance effect exhibited in memristors not only involves a complex memory of system variables, but also has its own complex nonlinear evolution. Memristors can act as a new type of synapse and play an important role in neuron dynamics [27,28].

These nonlinear electromagnetic constraint relationships, such as exponential function constraints, trigonometric and inverse trigonometric function constraints, hyperbolic functions, and multi-piecewise linear functions, exhibit complex divergent characteristics, or they may also show certain periodicity. Some have certain characteristics of activation functions, while others can be directly characterized as combinations of multiple linear relationships. Understanding the characteristics of these nonlinear functions can provide clearer insight into the role of complex nonlinear feedback in the generation and regulation of chaos, offering more choices of devices and schemes for the generation and fine-tuning of chaos. Below, taking these several nonlinear feedback functions as examples, we introduce this complex nonlinear feedback into a chaotic system to demonstrate its special function in chaos regulation.

### 2.2. Effect of Complex Nonlinear Feedback on Strange Attractors in a Chaotic System

In the following section, we take the offset-boostable chaotic system VB5 [29] as an example to illustrate the impact of different feedback terms on the chaotic attractor. The equation of the VB5 system is:

$$\begin{cases} \dot{x} = ayz, \\ \dot{y} = 1 - bz^2, \\ \dot{z} = x + yz + c. \end{cases} \quad (1)$$

Here, System (1) contains two non-bifurcation parameters, where parameter  $b$  is the amplitude parameter [30], parameter  $c$  is the offset boosting parameter for the  $x$ -dimension, and parameter  $a$  is the bifurcation parameter. To explore the impact of complex

nonlinear feedback on chaotic dynamics, we consider replacing the quadratic feedback term with other complex nonlinear functions, thus obtaining the general Equation (2) containing special nonlinear feedback terms.

$$\begin{cases} \dot{x} = ayz, \\ \dot{y} = 1 - f(z), \\ \dot{z} = x + yz + c. \end{cases} \quad (2)$$

Choosing different nonlinear functions  $f(z)$  allows us to observe the impact of complex nonlinear feedback on system dynamics and provides new options for the circuit implementation of different chaotic systems [31]. As shown in Table 1, eight different complex nonlinear feedback relationships are introduced here, and the corresponding function curves are shown in Figure 1. By adjusting the parameters  $a, b$  and  $f(z)$  in the system, chaotic attractors can be obtained. The system offset can be boosted by adjusting parameter  $c$ . The equilibrium points, eigenvalues, Lyapunov exponents, and initial values of these chaotic systems are also shown in Table 1, and the chaotic attractors are presented in Figure 2. The values of parameter  $b$  in Figure 1 are the same as those in Table 1.

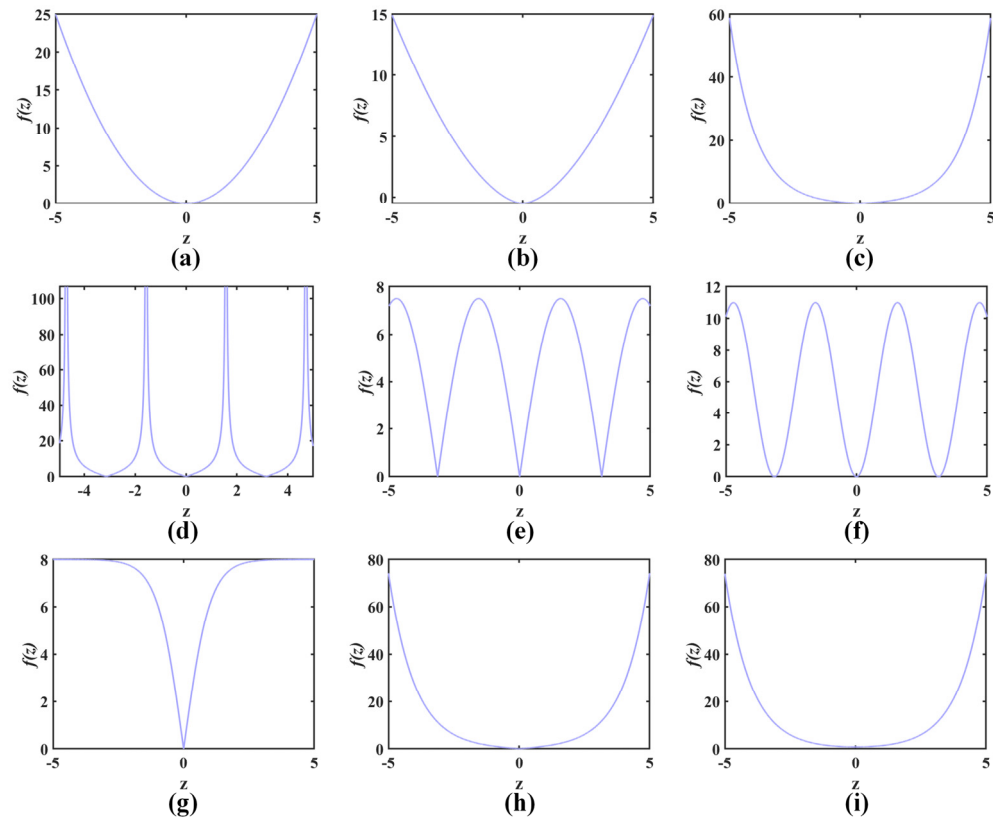


**Figure 1.** Curves of nonlinear feedback: (a)  $f(z) = bz^2$ , (b)  $f(z) = b|z|^{1.7} - 0.5$ , (c)  $f(z) = be^{-|z|} - 0.5$ , (d)  $f(z) = b|\tan z|$ , (e)  $f(z) = b|\sin z|$ , (f)  $f(z) = b \sin^2 z$ , (g)  $f(z) = b|\tanh z|$ , (h)  $f(z) = b \cosh(z) - 0.2$ , (i)  $f(z) = b|\sinh z|$ .

**Table 1.** Chaotic systems under complex nonlinear feedback.

Systems	$f(z)$	Parameters	Equilibria	Eigenvalues	x0 y0 z0	LEs	D <sub>KY</sub>
CSCF0	$bz^2$	$a = 1$	[0, 0, 1]	$-0.7709, 0.3855 \pm 1.5639i$	-1	(0.1394, -0.	
		$b = 1$	[0, 0, -1]	$-0.7709, 0.3855 \pm 1.5639i$	1	0002, -0.56	2.2454
CSCF1	$b z ^{1.7}-0.5$	$a = 1$	[0, 0, 1.2693]	$-0.6888, 0.3444 \pm 1.1856i$	-1	(0.2606, -0.	
		$b = 1$	[0, 0, -1.2693]	$-0.6888, 0.3444 \pm 1.1856i$	1	2239, -0.50	2.0729
CSCF2	$be^{ z }-0.5$	$a = 1$	[0, 0, 1.3217]	$-0.7698, 0.3849 \pm 1.5579i$	-1	(0.0868, -0.	
		$b = 0.4$	[0, 0, -1.3217]	$-0.7698, 0.3849 \pm 1.5579i$	1	0009, -0.52	2.1720
CSCF3	$b \tan z $	$a = 3.7$	[0, 0, 0.1399]	$-1.3376, 0.6688 \pm 1.5345i$	-1	(0.1609, -0.	
		$b = 5$	[0, 0, -0.1399]	$-1.3376, 0.6688 \pm 1.5345i$	1	0021, -0.92	2.1643
CSCF4	$b \sin z $	$a = 3.3$	[0, 0, $\arcsin \frac{2}{25}$ ]	$-1.0967, 0.5484 \pm 1.2251i$	-1	(0.1698, -0.	
		$b = 7.5$	[0, 0, $\arcsin \left(-\frac{2}{25}\right)$ ]	$-1.0967, 0.5484 \pm 1.2251i$	1	0017, -0.84	2.1993
CSCF5	$b\sin^2 z$	$a = 5$	[0, 0, $\arcsin \sqrt{\frac{1}{11}}$ ]	$-1.8310, 0.9155 \pm 2.1099i$	-1	(0.2534, -0.	
		$b = 11$	[0, 0, $\arcsin \left(-\sqrt{\frac{1}{11}}\right)$ ]	$-1.8310, 0.9155 \pm 2.1099i$	1	0007, -1.02	2.2454
CSCF6	$b \tanh z $	$a = 3.1$	[0, 0, $ar \tanh \frac{1}{8}$ ]	$-0.5647, 0.2823 \pm 0.5569i$	-1	(0.2037, -0.	
		$b = 8$	[0, 0, $ar \tanh \left(-\frac{1}{8}\right)$ ]	$-0.5647, 0.2823 \pm 0.5569i$	1	1058, -0.76	2.3544
CSCF7	$b\cosh(z)-0.2$	$a = 1$	[0, 0, $ar \cosh(1.2)$ ]	$-0.7854, 0.3927 \pm 1.6492i$	-1	(0.5423, -0.	
		$b = 1$			1	1976, -0.69	2.4948
CSCF8	$b \sinh(z) $	$a = 1$	[0, 0, $ar \sinh 1$ ]	$-1.6772, 0.8386 \pm 2.3293i$	-1	(0.1919, -0.	
		$b = 1$	[0, 0, $arsinh(-1)$ ]	$-1.6772, 0.8386 \pm 2.3293i$	1	0870, -0.63	2.1651
					-1	50)	

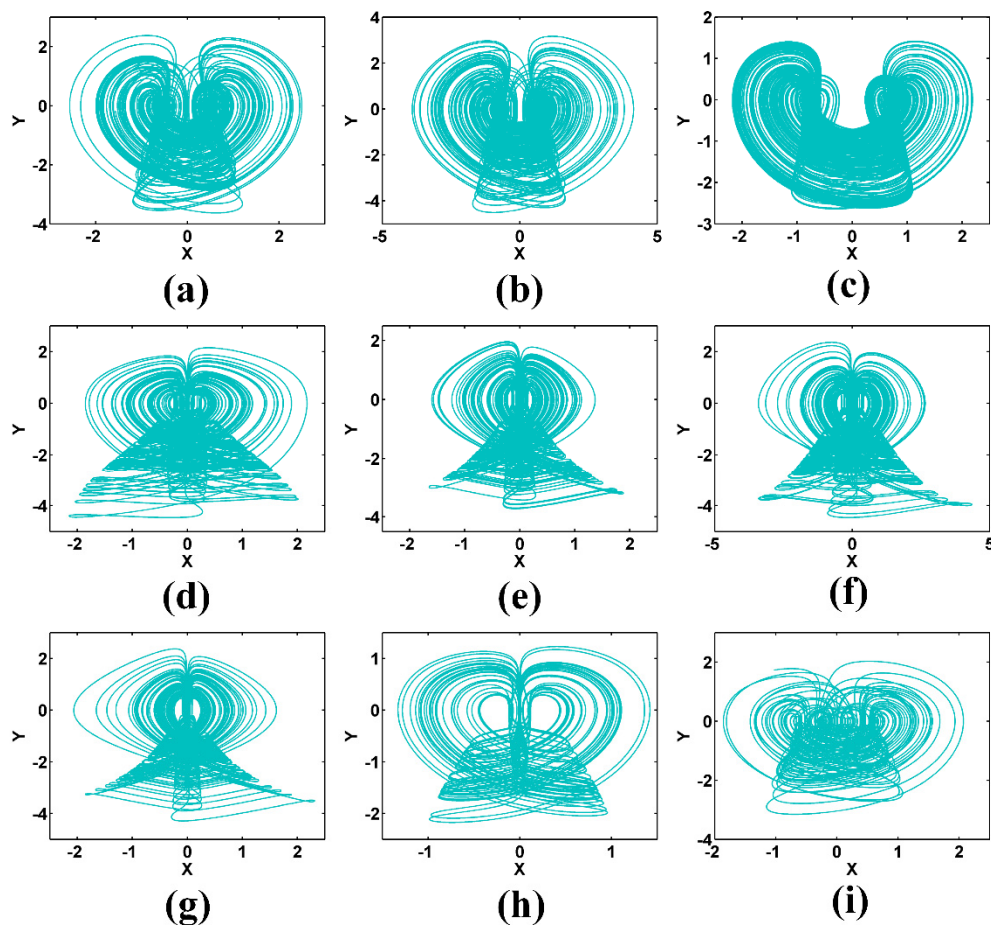


**Figure 2.** Projections of strange attractors in the  $x$ - $y$  plane corresponding to different nonlinear feedback: (a) CSCF0; (b) CSCF1; (c) CSCF2; (d) CSCF3; (e) CSCF4; (f) CSCF5; (g) CSCF6; (h) CSCF7; (i) CSCF8.

From Table 1, although the nonlinear feedback is different, when the system exhibits chaos, there are always two symmetrical equilibrium points, and the stability of the equilibrium points is the same, both being the saddle focus of index-2. Different nonlinear feedback causes the Lyapunov exponents of the corresponding chaotic attractors to show certain changes, among which the system CSCF7, generated by the nonlinear hyperbolic cosine function, has the largest Lyapunov exponent of the chaotic attractor. Different nonlinear feedback regulates the degree of intertwining between the twin-lobed attractors and changes the merging pattern of the twin-lobed attractors. We also note that there is only one nonlinear feedback term  $f(z)$  in the second dimension of System (2), so it is necessary to ensure that the value of  $f(z)$  is similar to the squared feedback in the original system CSCF0, that is, it is in the positive value interval. This requires adding an absolute value in the expression of  $f(z)$  to ensure its value is positive. If  $f(z)$  has multiple negative values or tendencies to zero, the corresponding system will become divergent in the second dimension due to too-strong positive feedback, or may even become unable to exhibit chaos.

From Figure 2, we can see that, although the introduction of different nonlinear complex feedback undoubtedly revises the attractor pattern and attractor domain, in general, it enriches the dynamical behavior.

### 3. Regulation of System Dynamics by Complex Nonlinear Feedback

#### 3.1. The Influence on the Non-Bifurcation Parameter of the System

General dynamical systems obtain corresponding chaotic attractors under specific parameters. However, these parameters are generally divided into bifurcation parameters and non-bifurcation parameters. Bifurcation parameters often trigger the transition of the system's dynamical behavior. When this parameter changes, the system switches from one dynamical behavior to another, such as from a fixed point to a periodic orbit, or even transitions to chaos or hyperchaos. Non-bifurcation parameters often cannot change the nature of the system's dynamical behavior. When this parameter changes, the system superficially maintains the same state and Lyapunov exponent, but the amplitude, average value, and other aspects of the system's output state variables will change. Sometimes, certain parameters in the system can change the amplitude and frequency of the system's state variables, achieving amplitude–frequency synchronization. At this time, although the Lyapunov exponent increases with the parameter, the corresponding parameter is still a non-bifurcation parameter because no bifurcation occurs.

The bifurcation parameters and non-bifurcation parameters in the system are not fixed. Different feedback networks can change the nature of parameters that were originally in the same position. For example, in the above System (1),  $a$  is a bifurcation parameter, while  $b$  and  $c$  are non-bifurcation parameters,  $b$  is a partial amplitude controller, and  $c$  is an offset parameter. Below, we explore the property revision of parameters when the nonlinear quadratic term in the system is replaced with other complex nonlinear functions, or the regulatory function of non-bifurcation parameters.

Case 1: The remaining function within the non-bifurcation amplitude controller

In system CSCF1, when special nonlinear power feedback is introduced, although the amplitude control function of the  $b$  parameter has not changed, the scale of its amplitude control is altered. The system equation for CSCF1 is:

$$\begin{cases} \dot{x} = ayz \\ \dot{y} = 1 - (b|z|^{1.7} - 0.5) \\ \dot{z} = x + yz \end{cases} \quad (3)$$

When an equivalent transformation  $x \rightarrow \sqrt[1.7]{\frac{1}{b}}x$ ,  $y \rightarrow y$ ,  $z \rightarrow \sqrt[1.7]{\frac{1}{b}}z$  is applied to

the above system, Equation (3) becomes:

$$\begin{cases} \dot{x} = ayz \\ \dot{y} = 1 - (|z|^{1.7} - 0.5) \\ \dot{z} = x + yz \end{cases} \quad (4)$$

It can be seen that the changing in parameter  $b$  causes the amplitude of system variables  $x$  and  $z$  to change. The system parameter  $b$  achieves partial amplitude control of  $x$  and  $z$ , with an amplitude control scale of  $\sqrt[1.7]{\frac{1}{b}}$ . In system CSCF1, when the parameter

$b$  changes within  $(0, 5]$ , the corresponding Lyapunov exponent and bifurcation parameter evolution are shown in Figure 3, while the amplitude control effects produced by different parameters  $b$  can be further illustrated by the phase trajectories and waveforms under two different parameters, as shown in Figure 4 and Figure 5, respectively.

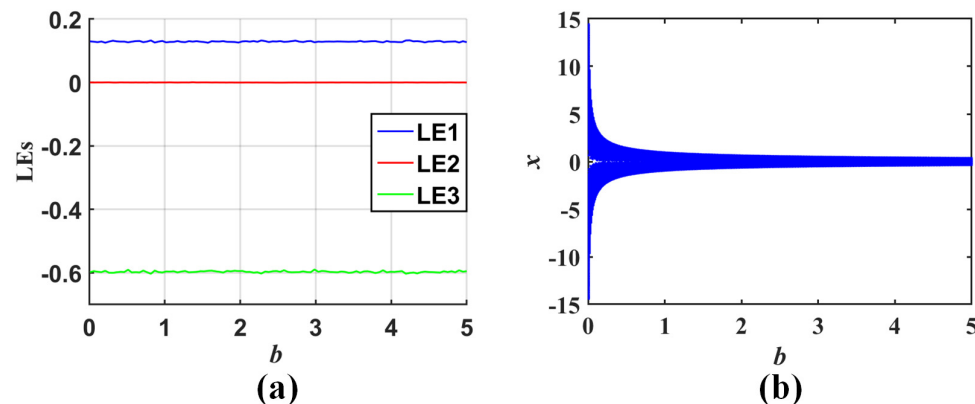


**Figure 3.** Non-bifurcation evolution under the amplitude controller  $b$  of the system CSCF1: (a) Lyapunov exponents, (b) bifurcation diagram.

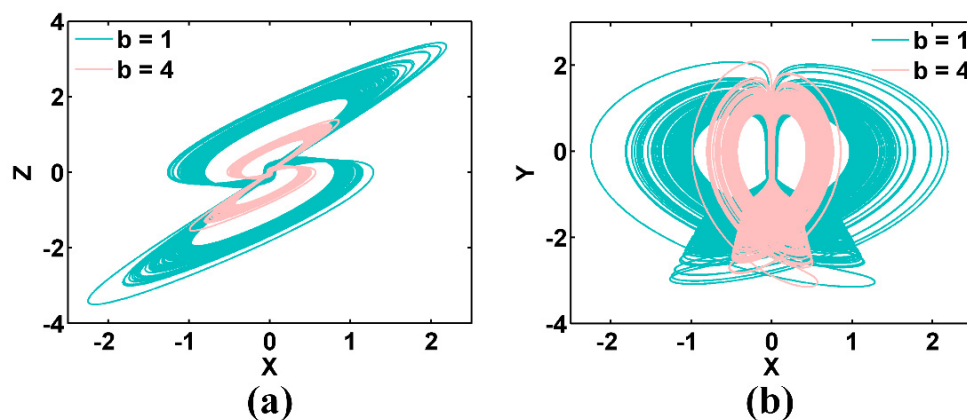


**Figure 4.** Phase trajectories of the system CSCF1 for different parameters  $b$ : (a) X-Z projection; (b) X-Y projection.

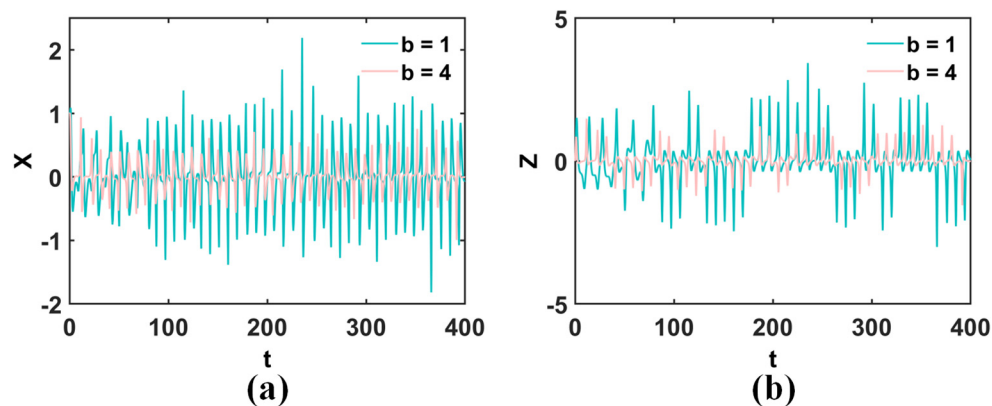


**Figure 5.** Waveforms of the system CSCF1 when parameter  $b$  is varied: (a)  $X(t)$ ; (b)  $Z(t)$ .

Case 2: Non-bifurcation amplitude controller turns to be a bifurcation parameter

Sometimes, the introduction of different nonlinear feedback functions can also change the nature of the non-bifurcation amplitude control parameter  $b$ . At this time, the non-bifurcation parameter may become a bifurcation parameter, but at the same time, the parameter region for bifurcation regulation may also embed local amplitude control attributes, and even achieve fine-tuning of amplitude and frequency within a certain local range. For example, by introducing a nonlinear hyperbolic sine function into the system,

the parameter  $b$  in the corresponding system CSCF8 will become a bifurcation parameter. This variable can regulate the system dynamics, causing it to transition from a periodic state to a chaotic state, as shown in Figure 6. However, at the same time, parameter  $b$  can regulate the amplitude–frequency relationship, which can be proven by the slightly linearly increasing Lyapunov exponent and bifurcation diagram. As shown in Figure 6, although the system presents a stable periodic oscillation state when  $b$  is between 0 and 0.75, when  $b$  increases from 0.83 to 2.6, the system presents a stable chaotic state, and its Lyapunov exponent slowly increases with parameter  $b$ . The amplitudes of the corresponding  $x$  and  $z$  state variables decrease synchronously with parameter  $b$ , indicating that in this local range, the system parameter  $b$  plays a role in amplitude and frequency control. However, when  $b$  further increases and exceeds 2.6, the system presents the same Lyapunov exponent, indicating that the divergence degree of the system state variables will no longer change at this time.

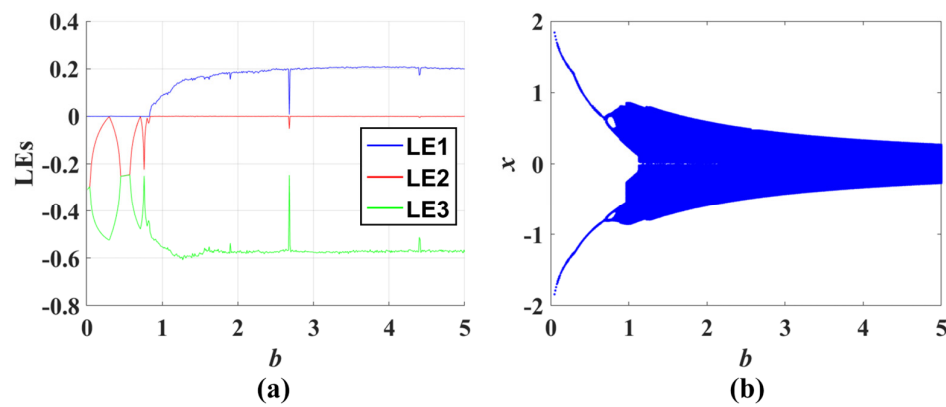


**Figure 6.** Dynamical evolution in system CSCF8 under parameter  $b$ : (a) Lyapunov exponents, (b) bifurcation diagrams.

In some cases, the difference in nonlinear feedback terms may directly transform a non-bifurcation parameter into a bifurcation parameter, such as in system CSCF7, where the introduction of the nonlinear hyperbolic cosine function causes the corresponding position of the  $b$  parameter to play a role in bifurcation regulation. The system frequently switches between multiple different periodic states and chaotic states, and the corresponding Lyapunov exponent and bifurcation diagram are shown in Figure 7.

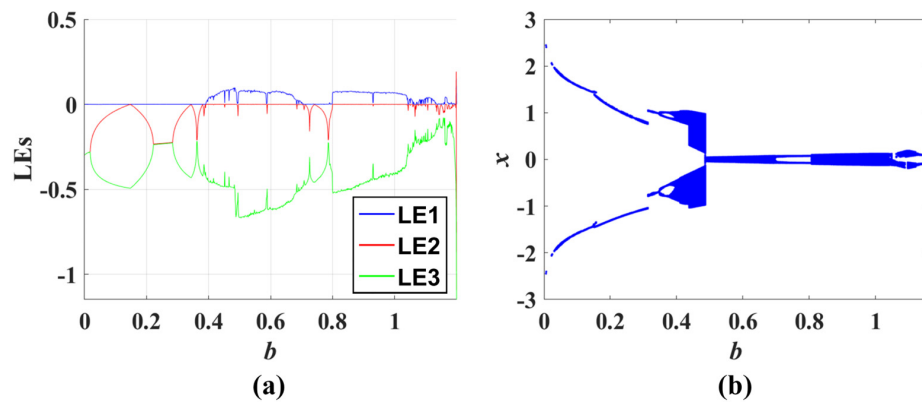


**Figure 7.** Partial amplitude and frequency control function of parameter  $b$  in system CSCF7: (a) Lyapunov exponent, (b) bifurcation diagrams.

Case 3: Offset parameter modified by nonlinear feedback

After substituting  $x$  with  $x - c$  into the system Equation (2), the parameter  $c$  in the system equation will disappear, which shows that the parameter  $c$  in the system equation achieves the offset boosting of the system variable  $x$ . Since the nonlinear function introduced in the second dimension of the system is only related to the state variable, the nonlinear feedback function at this time will not change the boosting effect of the non-bifurcation parameter  $c$ . However, since the amplitude control parameter has realized the regulation of the geometric size of the attractor, and the offset control has realized the transfer of the attractor in the phase space, the boosting process may exist independently of the amplitude control parameter. For example, in the system CSCF0, let

$x \rightarrow \frac{x}{\sqrt{b}} - c, y \rightarrow y, z \rightarrow \frac{z}{\sqrt{b}}$ , and the system turns to be:

$$\begin{cases} \dot{x} = ayz \\ \dot{y} = 1 - z^2 \\ \dot{z} = x + yz \end{cases} \quad (5)$$

In system CSCF1, let  $x \rightarrow \sqrt[1.7]{\frac{1}{b}}x - c, y \rightarrow y, z \rightarrow \sqrt[1.7]{\frac{1}{b}}z$ , and the system turns to:

$$\begin{cases} \dot{x} = ayz \\ \dot{y} = 1 - (|z|^{1.7} - 0.5) \\ \dot{z} = x + yz \end{cases} \quad (6)$$

Returning to the original systems CSCF0 and CSCF1, when  $b = 1, c = 0$  and  $b = 2, c = 5$ . The phase trajectories of the two systems are shown in Figure 8.

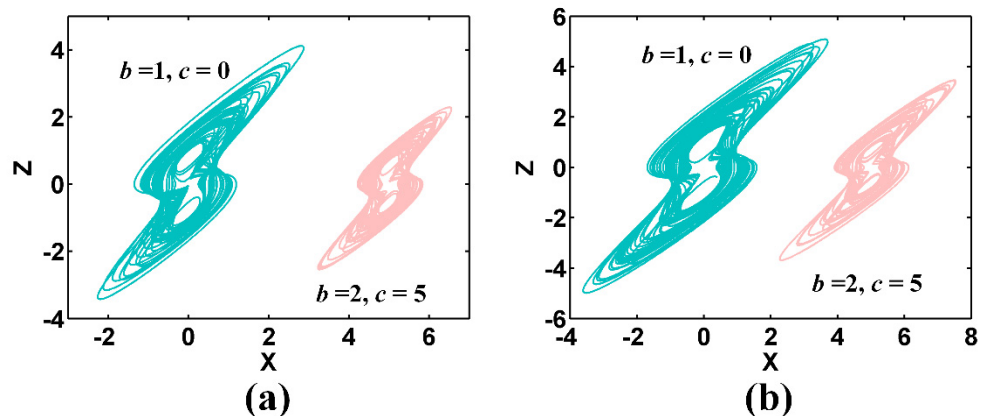


**Figure 8.** Projections of the phase trajectories of systems CSCF0 and CSCF1 in the  $x$ - $z$  plane for  $b = 2, c = 5$  and  $b = 1, c = 0$ : (a) CSCF0; (b) CSCF1.

### 3.2. The Influence of Complex Nonlinear Feedback on Bifurcation Parameters

Different nonlinear feedback terms can also affect the bifurcation parameters of the system. For ease of observation, here, we first present the coexisting dynamical behaviors when the bifurcation parameter  $a$  of system CSCF0 evolves, as shown in Figure 9. Under the action of symmetric initial values, the bifurcation behavior of the system exhibits symmetry; thus, the system has bistable properties. The coexisting attractors of the system under specific parameters and the signal waveform are shown in Figure 10. We notice that if the attribute of the non-bifurcation amplitude control parameter is preserved, the attribute of the bifurcation

parameter also remains almost unchanged. Here, we observe the bifurcation and Lyapunov exponent spectrum when the parameter of system CSCF1 evolves, and we find that system CSCF1 exhibits almost similar dynamical behavior to CSCF0, as shown in Figure 11. Here, even with the number of times the periodic window appears, the parameters are almost close. The symmetric coexisting behavior exhibited by system CSCF1 is shown in Figure 12.

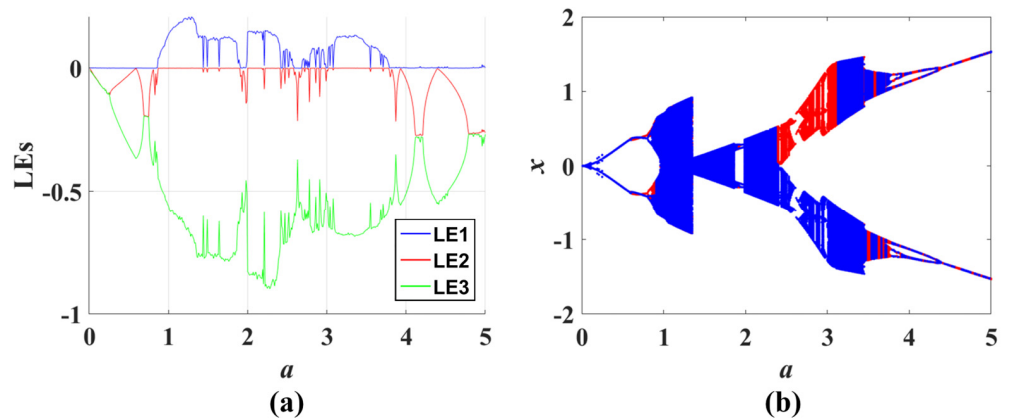


**Figure 9.** Dynamic evolution of CSCF0 when parameter  $a$  varies: (a) Lyapunov exponents, (b) bifurcation diagram. Initial conditions (IC) are: ICs =  $[-1, 1, -1]$  (blue), ICs =  $[1, 1, 1]$  (red).

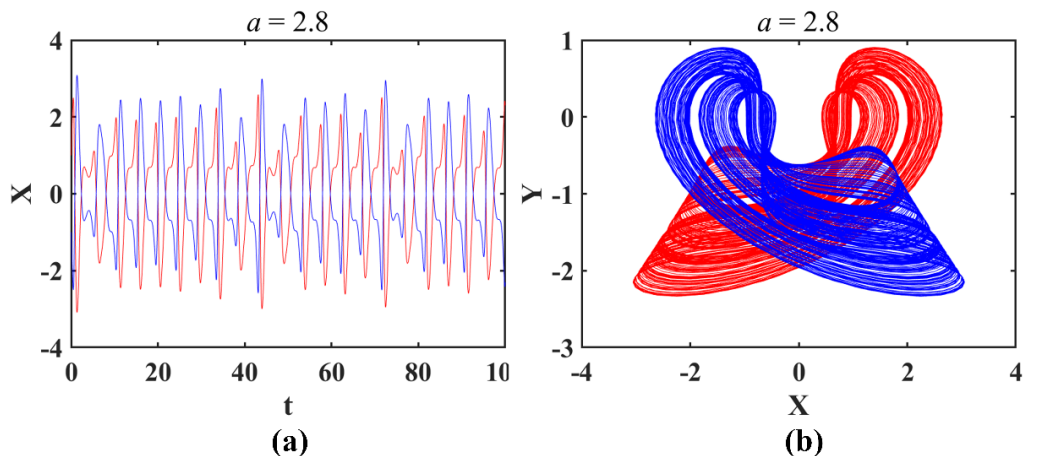


**Figure 10.** Coexisting solutions of CSCF0: (a)  $X(t)$ , (b) the projection in the  $x$ - $y$  plane. ICs =  $[-1, 1, -1]$  (blue), ICs =  $[1, 1, 1]$  (red).

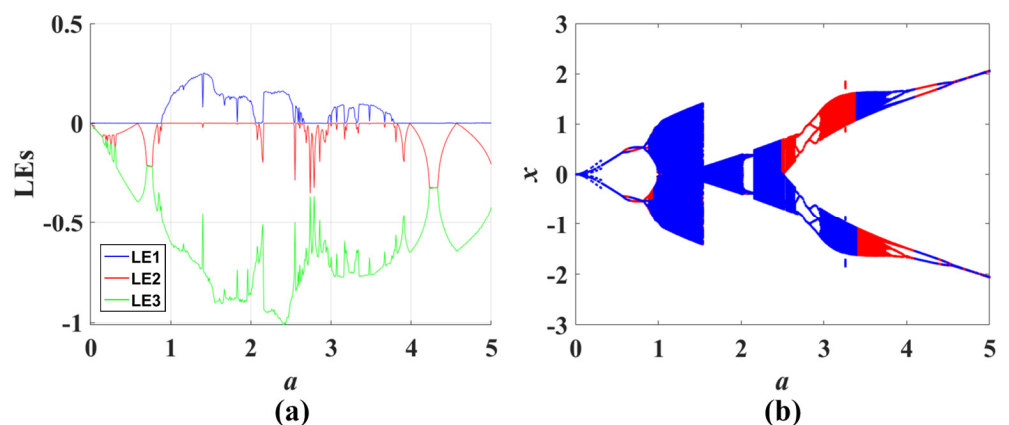


**Figure 11.** Coexisting evolutions of CSCF1 as parameter  $a$  is varied: (a) Lyapunov exponents, (b) bifurcation diagram. ICs =  $[-1, 1, -1]$  (blue), ICs =  $[1, 1, 1]$  (red).

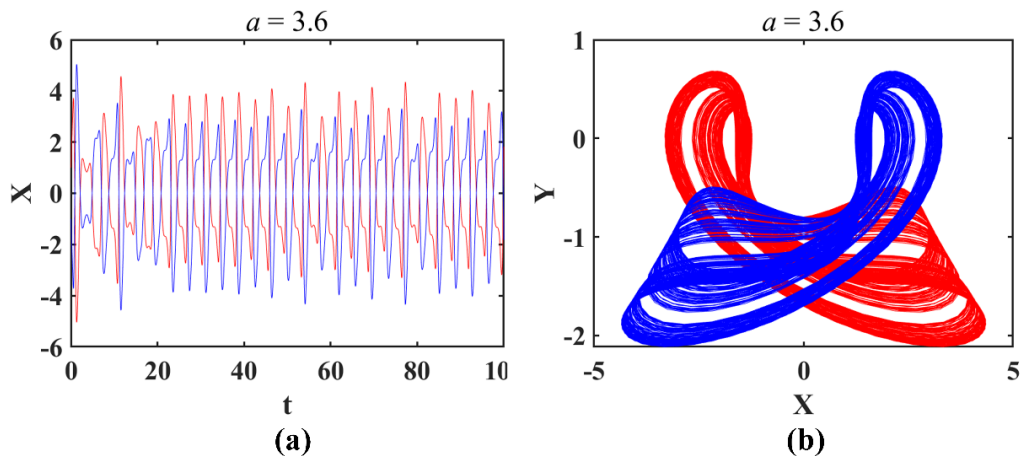


**Figure 12.** Coexisting solutions of CSCF1 as parameter  $a$  is varied: (a)  $X(t)$ , (b) the phase tracks in the  $x$ - $y$  plane. ICs =  $[-1, 1, -1]$  (blue), ICs =  $[1, 1, 1]$  (red).

Furthermore, it can be found that attractors of CSCF5-7, shown in Figure 2, share the same slim-waist-like structure. This structure is caused by the feedback of a nonlinear function with a steep slope (See Figure 1). Therefore, here, taking system CSCF5 as an additional example, the bifurcation and Lyapunov exponent spectra of the system expose the evolution of its coexisting dynamics, as shown in Figure 13. The dynamic behavior is like that of CSCF0 when the parameter  $a$  is within  $[0, 5]$ . The symmetric coexisting behavior is further shown in Figure 14.

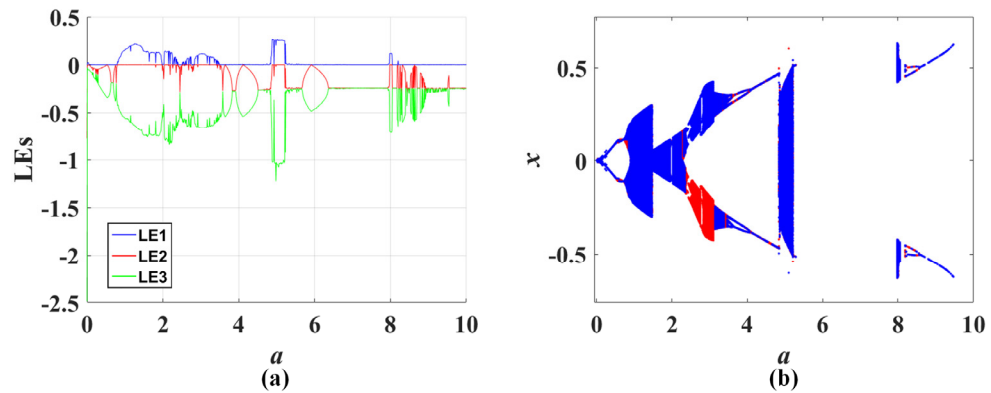


**Figure 13.** Coexisting evolutions of CSCF6 as parameter  $a$  is varied: (a) Lyapunov exponents, (b) bifurcation diagram. ICs =  $[-1, 1, -1]$  (blue), ICs =  $[1, 1, 1]$  (red).

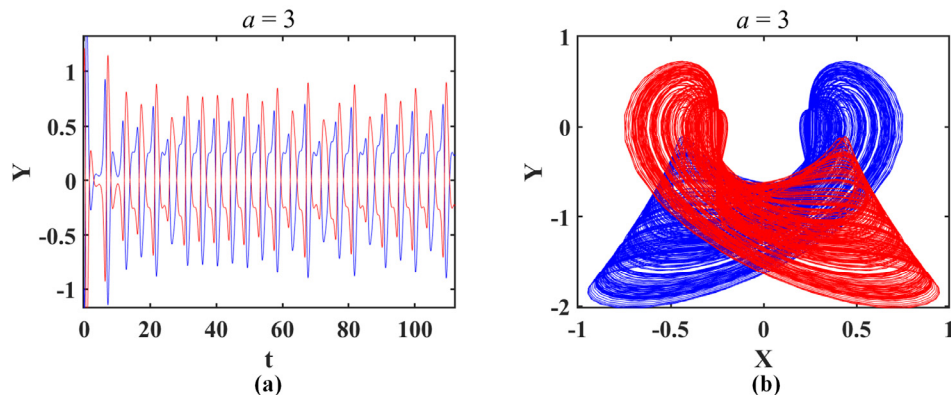


**Figure 14.** Coexisting solutions of CSCF6 as parameter  $a$  is varied: (a)  $Y(t)$ , (b) the phase tracks in the  $x$ - $y$  plane. ICs =  $[-1, 1, -1]$  (blue), ICs =  $[1, 1, 1]$  (red).

In many cases, the introduction of complex nonlinear feedback terms will change the bifurcation behavior of the system, and sometimes even introduce more unexpected multistable phenomena. As shown by system CSCF8, the dynamics under the change of the corresponding bifurcation parameter  $a$  are shown in Figure 15. At this time, the parameter interval in which the system presents a chaotic state is completely different from the previous two systems, CSCF1 and CSCF0. In addition to the difference in the size of the Lyapunov exponent, there is also a difference in the chaotic region. In system CSCF8, there is also a phenomenon of multiple attractors coexisting with chaos and two periodic states, as shown in Figure 16, but this coexistence is also a common situation when symmetry is broken. Here, it just shows that chaotic systems under different nonlinear feedback have different stabilities.

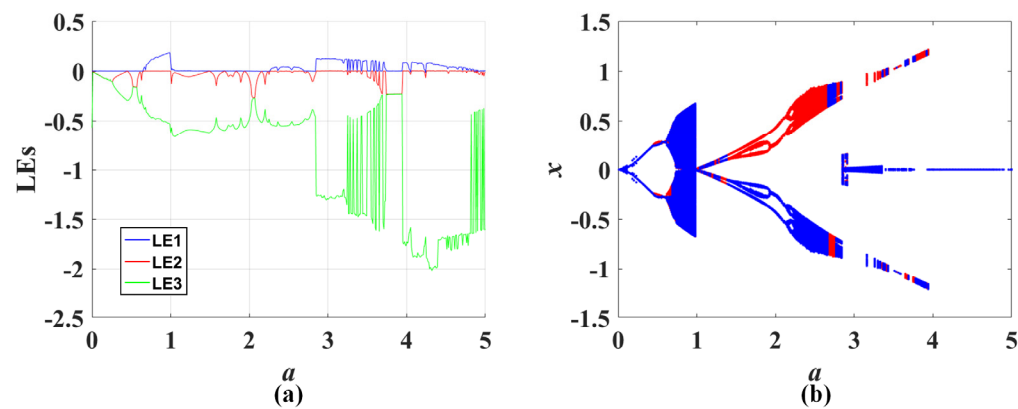


**Figure 15.** Dynamic evolutions of CSCF8 when the parameter  $a$  is varied: (a) Lyapunov exponent, (b) bifurcation diagram. ICs =  $[-1, 1, -1]$  (blue), ICs =  $[1, 1, 1]$  (red).

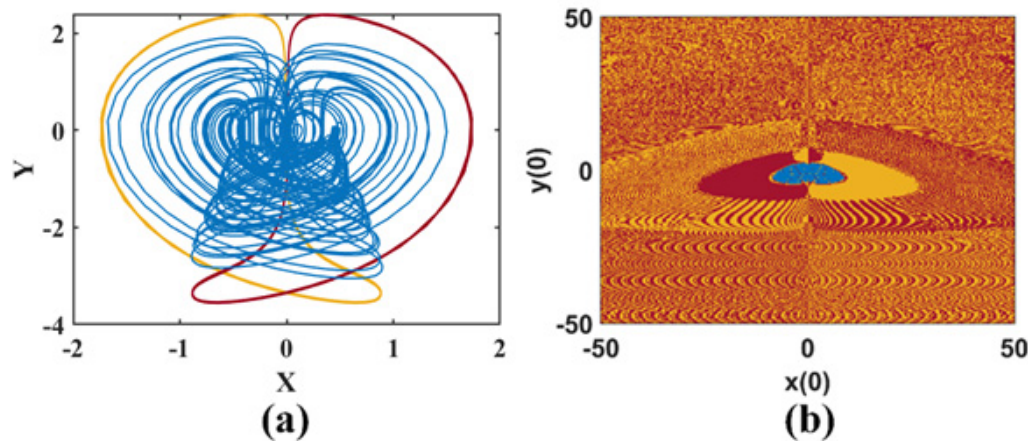


**Figure 16.** Coexisting attractors of CSCF8 with  $a = 1$ ,  $b = 1$  and their corresponding basins of attraction: (a) coexisting periodic and chaotic states. ICs =  $[-1, 1, -1]$  (blue), ICs =  $[1, 0, 0]$  (red), ICs =  $[-1, 0, 0]$  (yellow). (b) Basin of attraction in the  $x(0)$  -  $y(0)$  plane ( $z(0) = 0$ ).

Even without the introduction of multistability, the impact of the bifurcation parameter  $a$  on the system's dynamical behavior can undergo significant changes due to the introduction of special nonlinear functions, generally leading to the introduction of more diverse forms of chaotic states. For example, in system CSCF7, when the parameter  $a$  changes at 0.38, the system enters a chaotic state from a period bifurcation, as shown in Figure 17. When  $a$  is greater than 0.59, the system presents a variable chaotic state, with different attractors having different extension and contraction scales in phase space.

However, its convergence requirements are continuously increasing, which manifests as the Lyapunov exponent remaining unchanged in the positive direction while increasing in the negative direction. This means that the divergence of a certain dimension requires greater convergence strength from other dimensions to maintain the existence of the chaotic attractor. Some typical phase trajectories which were observed are shown in Figure 18.

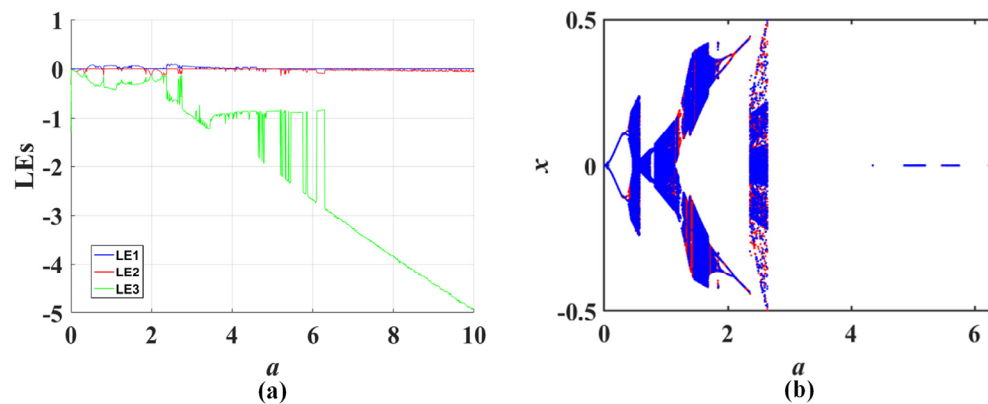


**Figure 17.** Dynamic evolution of CSCF7 as parameter  $a$  is varied: (a) Lyapunov exponents, (b) bifurcation diagram. ICs =  $[-1, 1, -1]$  (blue), ICs =  $[1, 1, 1]$  (red).

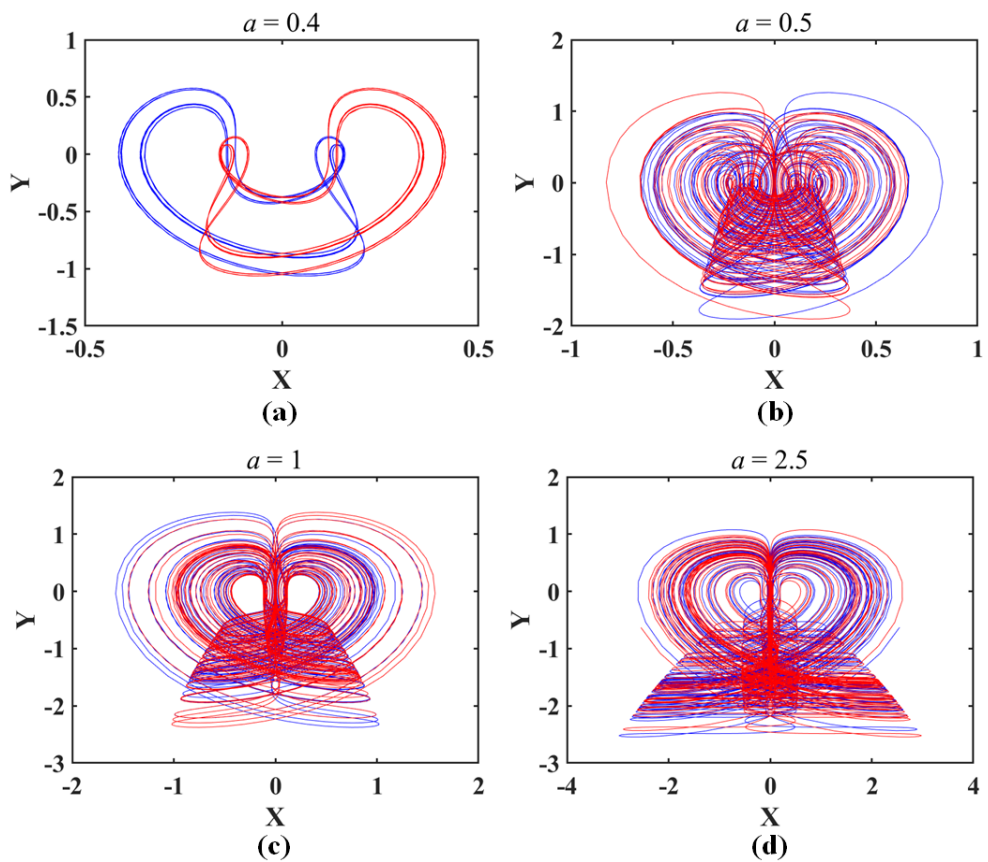


**Figure 18.** Typical phase trajectory of CSCF7 under specific parameter  $a$ . (a)  $a=0.4$  (b)  $a=0.5$  (c)  $a=1$  (d)  $a=2.5$ . ICs =  $[-1, 1, -1]$  (blue), ICs =  $[1, 1, 1]$  (red).

Different complex nonlinear feedback terms in the system may revise the function of the original bifurcation parameter and non-bifurcation parameter in the system. From the

above analysis, there are some clues for system design when selecting nonlinear complex function for the feedback:

- (1) Steep feedback with a large slope could tie a knot on the attractor, making the attractor form a slim-waist-like structure (Figures 1d–g and 2d–g).
- (2) Attractor size expansion/reduction can be realized by adjusting the parameter  $b$  in systems CSCF0 and CSCF1. The other feedback of the complex function causes the parameter  $b$  to become a bifurcation parameter, although, in some numerical range, it can modify the attractor size, such as in CSCF8.
- (3) The symmetry of complex feedback functions provides the possibility of coexisting attractors in chaotic systems with this structure (shown in Figures 9, 11, 13, 15 and 17), and wide-mouth-like feedback can even bring three or more coexisting attractors, like system CSCF8 (shown in Figure 16).
- (4) All the systems (CSCF0–CSCF8) have a single parameter  $c$  in the last dimension, leading to direct offset boosting of the variable  $x$ .
- (5) The impact of complex nonlinear feedback on system dynamics is reflected in the transition between non-bifurcation parameters and bifurcation parameters, as well as the bifurcation dynamics. The transition from the non-bifurcation parameter to the bifurcation one when the original system is introduced to new complex feedback usually does not cause structural rupture or deformation of the attractor. Therefore, there are no coexisting attractors generated as a result (as shown in Figures 6 and 7). For the bifurcation parameters, after introducing complex functions, all the derived systems retain the original basic bifurcation patterns, including the generation of coexisting attractors (shown in Figures 9, 11, 13, 15, and 17).

## 4. Circuit Realization Based on FPAA

### 4.1. FPAA Internal Resources and System Scale Transformation

The FPAA is a highly programmable analog integrated circuit that allows for on-site configuration of the functionality and connections of analog circuits. Similarly to the Field Programmable Gate Array (FPGA), the FPAA provides a flexible configuration method to implement various analog circuits. The core of the FPAA is a series of Programmable Analog Modules (PAMs), each containing analog circuit components such as operational amplifiers, capacitors, comparators, etc., which can be configured and adjusted according to design requirements to meet specific performance indicators and functional needs. However, the traditional FPAA often faces high circuit initialization complexity when dealing with circuits with initial values, which are very important for chaotic circuit systems. To solve this problem, a Digital Programmable Analog Signal Processor (DPASP) was introduced to reduce initialization difficulty and improve system performance. DPASP is a device that combines digital technology with analog signal processing capabilities. It is similar to a traditional FPAA, but introduces digital technology on top of it to enhance flexibility and efficiency when processing analog signals. Through DPASP, the dynamic configuration of signal processor can be realized, the complexity of circuit initialization can be reduced, and the initial value of a circuit system can be configured accurately and quickly.

In this paper, two Anadigm DualApex development boards containing AN231E04 chips are used to build systems CSCF0–CSCF8, outputting chaos under any non-zero initial state. An AN231E04 chip internally contains four CBA modules, which can be configured through the design software AnadigmDesigner 2 to implement corresponding functions by configuring operational amplifiers, capacitors, comparators, and other circuit components in the modules. Since DPASP has a differential output voltage of  $\pm 3$  V, voltage values exceeding this range will be locked at  $\pm 3$  V, so it is necessary to scale each

system CSCF0-8 separately to ensure that the voltage is always within the  $\pm 3$  V range, guaranteeing that the designed circuit can work properly.

Taking system CSCF0 as an example, by observing the attractor, it is necessary to scale down the equation variables  $x, y, z, \dot{x}, \dot{y}, \dot{z}$  and scale the system accordingly to obtain Equation (7).

$$\begin{cases} \dot{x} = 6ayz \\ \dot{y} = \frac{1}{6} - \frac{(5z)^2}{6} \\ \dot{z} = x + 6yz \end{cases} \quad (7)$$

The scaled phase trajectory is shown in Figure 19.

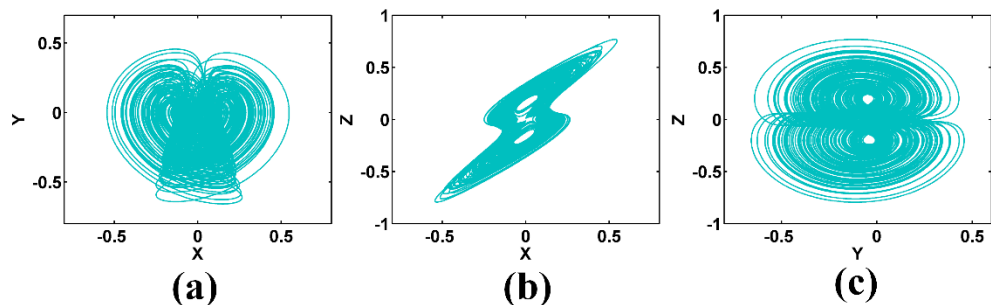


**Figure 19.** Projections of the chaotic attractor of the rescaled system CSCF0 on different planes: (a) X-Y plane; (b) X-Z plane; (c) Y-Z plane.

To facilitate implementation on the FPA platform, other chaotic systems, i.e., CSCF1-CSCF8, also need to undergo scaling, and the corresponding scaling factors are shown in Table 2. It should be noted that, since the initial values also have a significant impact on the chaotic system, the initial values of the corresponding system variables also need to be scaled accordingly.

**Table 2.** Scaling transformations for chaotic systems containing complex nonlinear feedback.

System	System Scaling Ratio	System	System Scaling Ratio
CSCF1	$x \rightarrow 6x, y \rightarrow 8y, z \rightarrow 5z$	CSCF2	$x \rightarrow 5x, y \rightarrow 10y, z \rightarrow 5z$
CSCF3	$x \rightarrow 6x, y \rightarrow 10y, z \rightarrow 2z$	CSCF4	$x \rightarrow 4x, y \rightarrow 3y, z \rightarrow 2z$
CSCF5	$x \rightarrow 10x, y \rightarrow 10y, z \rightarrow 5z$	CSCF6	$x \rightarrow 5x, y \rightarrow 3y, z \rightarrow 2z$
CSCF7	$x \rightarrow 2x, y \rightarrow 3y, z \rightarrow 2z$	CSCF8	$x \rightarrow 4x, y \rightarrow 5y, z \rightarrow 4z$

#### 4.2. Circuit Implementation Based on FPA

The implementation of the analog chaotic circuit requires selecting and configuring chip parameters in the design software AnadigDesigner 2, as well as setting the weights of different CAM devices. Since the basic equation structures of systems CSCF0–CSCF8 are the same, with the difference being only in the parameters  $a, b$  and the complex nonlinear function  $f(z)$ , it is only necessary to modify some CAM devices and their weights to implement systems CSCF0-CSCF8. Considering that the initial values of each system are not zero, it is necessary to use the dynamic routing configuration function of FPA [32]. Figure 20 is the block diagram of the FPA system. For ease of analyzing logical relationships and distinguishing variables, green lines represent variable  $x$ , yellow lines represent variable  $y$ , and brown lines represent variable  $z$ . Combining the principle of dynamic configuration routing of FPA, the entire system block diagram can be

divided into two modules—the integrator charging module (system1\_ic and system2\_ic) and the chaotic circuit implementation module (system1 and system2). The integrator charging module mainly sets the initial values of the chaotic system, while the chaotic circuit implementation module operates on the set initial values of the chaotic system and outputs chaotic waveforms. The wiring connection between the two chips (system1\_ic and system2\_ic) in the integrator charging module is consistent with the wiring connection between the two chips (system1 and system2) in the chaotic circuit implementation module. In addition, the I/O configuration methods in both modules are also consistent. The difference between the two modules is that in the integrator charging module, the integrator in system2\_ic is not connected to the variable output by system1\_ic, but is connected to its internal negative feedback adder, while in the chaotic circuit implementation module, the integrator in system2 is connected to the variable output by system1. The system2\_ic in the integrator charging module implements integrator charging, thereby completing the setting of the initial values of the chaotic system. By controlling the value of the constant  $b$ , the integrator is charged to the desired initial value  $x_0$ . In AnadigDesigner 2, only the Voltage ( $\pm 2$  V) CAM device can realize a fixed constant, which cannot change parameter  $x_0$ . It is necessary to control the multiplier coefficient  $k$  of the corresponding adder to achieve the setting of  $x_0$ , and it is necessary to satisfy the multiplier coefficient  $k = b/2$ .

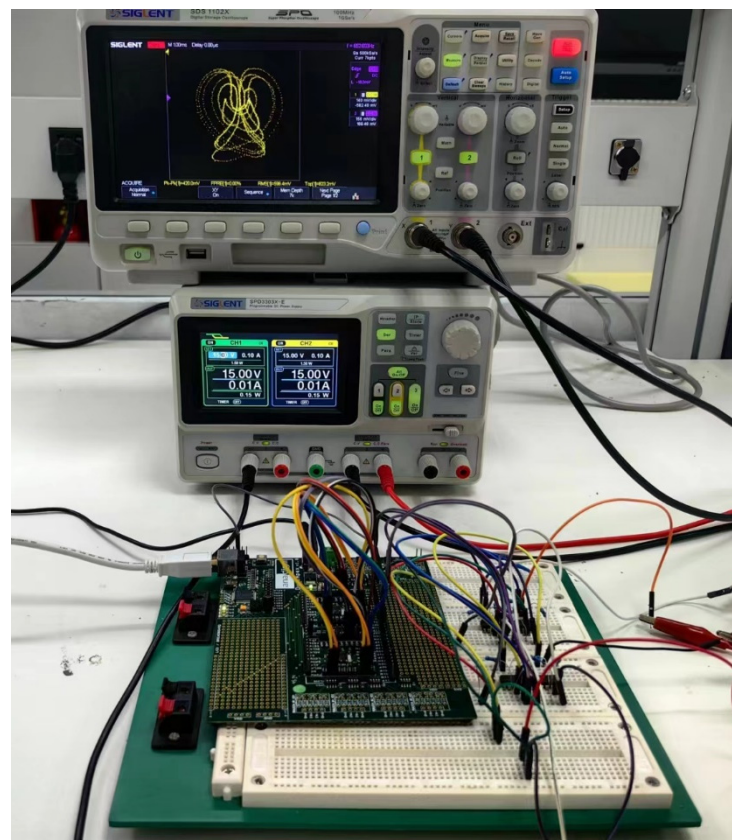


**Figure 20.** Hardware diagram of the FPAA development board.

The FPAA system can be simply divided into fixed CAM devices and adjustable CAM devices. The parameters and settings of the fixed CAM devices remain unchanged, and the settings of the adjustable CAM devices remain unchanged. By modifying some parameters in the adjustable CAM devices, systems CSCF0–CSCF8 can be implemented. The specific CAM device parameter configuration refers to Tables 3–7, where the shaded

parameters in Tables 3 and 4 are the adjustable parameters of the adjustable CAM devices, and their corresponding values in each system are recorded in Tables 5–7.

**Table 3.** Device parameter configuration of system1\_ic (system1) CAM.

Name	Options	Parameters	Clocks
Multiplier	Sample and Off: Off Output Phase: Phase 1 Input 1: Non-inverting Input 2: Non-inverting Input 3: Off Input 4: Off Output Phase: Phase 1 Input 1: Non-inverting Input 2: Inverting Input 3: Off Input 4: Off	Multiplication Factor: 0.333 Gain 1: Num1 Gain 2: Num2 Gain 1:Num3 Gain 2:Num4	ClockA:250 kHz ClockB:4 MHz ClockA:250 kHz ClockA:250 kHz
SumDiff(1)			
SumDiff(2)			
Voltage	Polarity Positive (+2 V)		
GainHalf	Polarity: Non-inverting Input Sampling Phase: Phase 1 Input Sampling Phase: Phase 1/2	Gain: Num5	ClockA:250 kHz
Hold	(The Phase depends on the output of the connected adder)		ClockA:250 kHz
TransferFunction	Output Hold: Off		ClockA:250 kHz ClockB:4 MHz

**Table 4.** Device parameter configuration of system2\_ic (system2) CAM.

Name	Options	Parameters	Clocks
Integrator(1) ~ (3)	Polarity: Non-inverting Input Sampling Phase: Phase 1 Compare Control To: No Reset Output Phase: Phase 1	Integration Const: 0.0025 [1/us]	ClockA:250 kHz
SumDiff(1)	Input 1: Inverting Input 2: Inverting Input 3: Off Input 4: Off Output Phase: Phase 1	Gain 1: $\frac{x_0}{2}$ Gain 2: 1.00	ClockA:250 kHz
SumDiff(2)	Input 1: Non-inverting Input 2: Inverting Input 3: Off Input 4: Off Output Phase: Phase 1	Gain 1: $\frac{y_0}{2}$ Gain 2: 1.00	ClockA:250 kHz
SumDiff(3)	Input 1: Inverting Input 2: Inverting Input 3: Off Input 4: Off Output Phase: Phase 1	Gain 1: $\frac{z_0}{2}$ Gain 2: 1.00	ClockA:250 kHz

**Table 5.** Adjustable CAM device parameter configuration of CSCF0-CSCF2.

CSCF0	CSCF1	CSCF2
Num 1	18	Num 1
Num 2	1	Num 2

Num 3	0.083	Num 3	0.09375	Num 3	0.075
Num 4	4.167	Num 4	1.25	Num 4	1
Num 5	18	Num 5	20	Num 5	10
$f(z)$	$z^2$	$f(z)$	$0.1 5z ^{1.7}$	$f(z)$	$0.04e^{ 5z }$

**Table 6.** Adjustable CAM device parameter configuration of CSCF3-CSCF5.

CSCF3		CSCF4		CSCF5	
Num 1	30	Num 1	9	Num 1	30
Num 2	3	Num 2	2	Num 2	2
Num 3	0.05	Num 3	0.167	Num 3	0.05
Num 4	1	Num 4	2.5	Num 4	1
Num 5	33	Num 5	13.85	Num 5	75
$f(z)$	$0.071 \tan(2z) $	$f(z)$	$ \sin(2z) $	$f(z)$	$\sin^2 z$

**Table 7.** Adjustable CAM device parameter configuration of CSCF6-CSCF8.

CSCF6		CSCF7		CSCF8	
Num 1	6	Num 1	9	Num 1	15
Num 2	2.5	Num 2	1	Num 2	1
Num 3	0.167	Num 3	0.2	Num 3	0.15
Num 4	2.667	Num 4	5	Num 4	2
Num 5	7.26	Num 5	9.3	Num 5	15
$f(z)$	$0.071 \tan(2z) $	$f(z)$	$ \sin(2z) $	$f(z)$	$\sin^2 z$

The TransferFunction function uses a lookup table to provide the corresponding implementation function. It calls a register in the chip, dividing the  $\pm 3$  V voltage into 256 equal parts, corresponding to 256 voltage access intervals. Each access interval stores a value within the range of  $\pm 3$  V. If the value exceeds the  $\pm 3$  V range, it will be locked at  $\pm 3$  V. When using the TransferFunction function, it is necessary to consider the voltage range and precision issues, that is, the value in the corresponding voltage value access interval is within  $\pm 3$  V and meets the 23 mV voltage interval. Therefore, it is generally necessary to appropriately scale the implemented function. The specific adjustable CAM period parameters of systems CSCF0-8 and the functions implemented by TransferFunction are shown in Tables 5–7.

After setting the circuit parameters, they need to be downloaded to the development board. The specific method is as follows: First, the main configuration AHF composed of system1\_ic and system2\_ic is downloaded to the development board, and then the dynamic configuration AHF file composed of system1 and system2 is downloaded as well. During this process, no additional operations are required, and the wiring and jumper caps on the development board must remain unchanged. Figure 21 is the FPAA framework diagram. The FPAA needs to be connected according to the architecture diagram. Since the FPAA outputs differential signals, an external subtractor is needed to output the correct waveform. Figure 22 is the phase trajectory diagram of the chaotic system actually output by the FPAA. It should be noted that, due to different oscilloscope sampling rates, sampling times, and other parameters, the output phase trajectory diagrams may also differ. The simulation parameter values can be appropriately adjusted according to the actual situation to solve this issue. Since the FPAA outputs a differential signal, it needs to pass through the subtracter to output the correct signal. Its circuit structure is shown in Figure 23. Ports 21 of system1 and system2 need to be connected to the Vp port of the subtracter, and all ports 22 need to be connected to the Vn port of the subtracter. In the circuit

schematic diagram, the model of the operational amplifier is LM741. The circuit element parameters are selected as follows:  $R_1 = R_2 = R_3 = R_4 = R_5 = 10\text{k}\Omega$ .

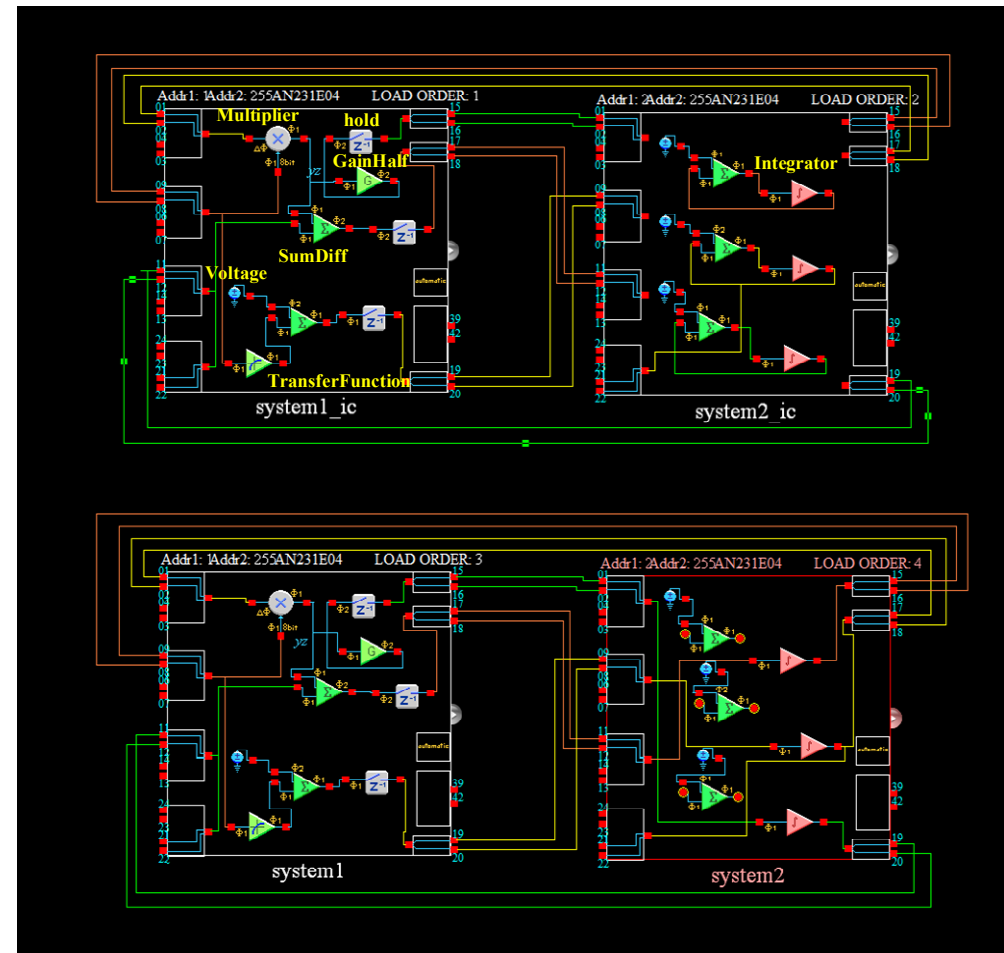


**Figure 21.** FPAA framework.

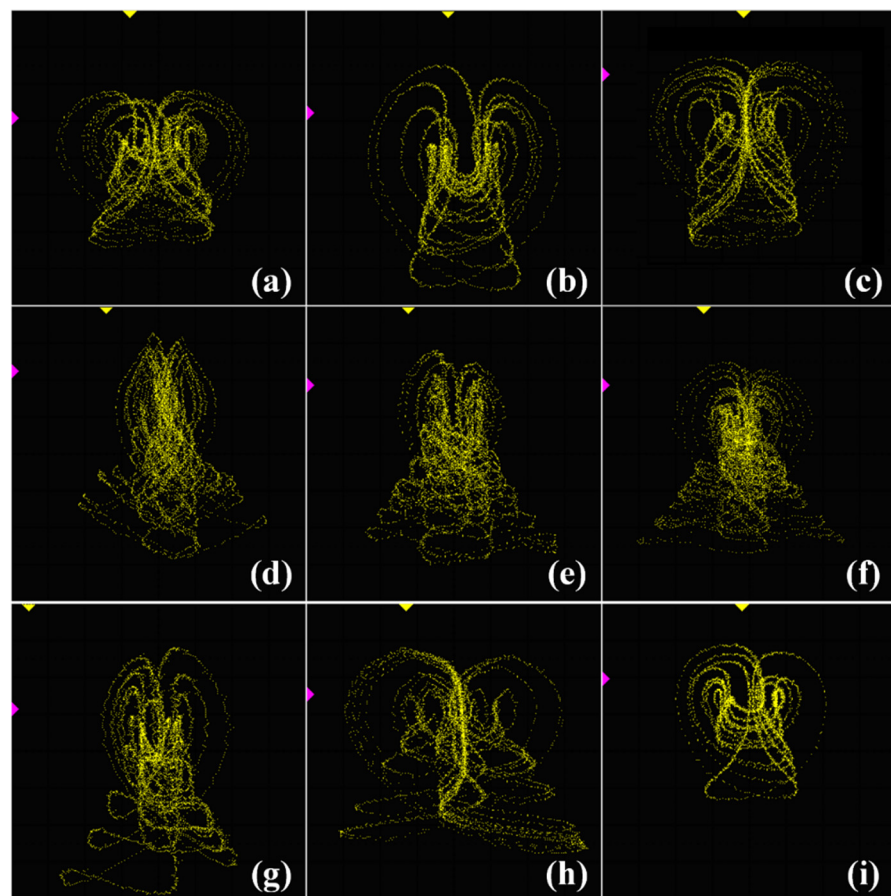


**Figure 22.** Phase trajectories of chaotic systems from actual output of FPAA. (a) CSCF0; (b) CSCF1; (c) CSCF2; (d) CSCF3; (e) CSCF4; (f) CSCF5; (g) CSCF6; (h) CSCF7; (i) CSCF8.

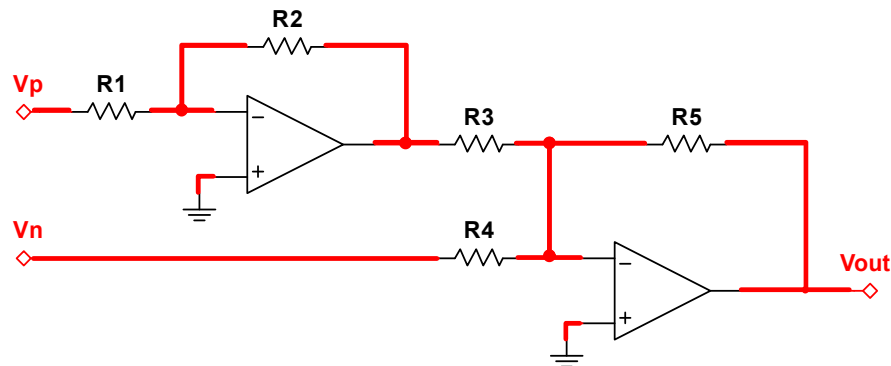


**Figure 23.** Circuit schematic of subtracter.

## 5. Discussion and Conclusions

This paper studies the impact of special nonlinear function feedback on system dynamics by introducing different complex nonlinear feedback. Specifically, by adjusting the nonlinear feedback terms, we further observe the changes in the regulatory effects of the original bifurcation parameters and non-bifurcation parameters in the system equation on the system's dynamic behavior. The introduction of special nonlinear feedback terms changes the properties of the original bifurcation parameters in the system over the system's dynamic behavior and further alters the regulatory effect of the original non-bifurcation parameters on the system's state variables.

Based on an offset-boostable chaotic system VB5, we introduced a variety of different nonlinear feedback functions to observe their actual regulatory effects on the system's dynamical behavior. It was found that nonlinear feedback functions can affect the portrait of attractors and their basins of attraction, as well as change the occurrence and evolution of chaos and even alter the regulatory role of non-bifurcation parameters. Through the FPAA platform, the impacts of various nonlinear function feedback on the system dynamics were verified, and all changes in the systems' dynamic behavior were observed. The circuit verification based on FPAA shortened the time required for circuit implementation, greatly reduced the complexity and difficulty of circuit implementation, and greatly improved the efficiency of chaotic system generation.

**Author Contributions:** J.X.: investigation, circuit implementation, data curation, and writing—original draft. C.L.: conceptualization, methodology, writing—review and editing, project administration, and funding acquisition. X.C.: validation and circuit implementation. X.Z.: software and writing—review and editing. L.C.: mathematical analysis and visualization. All authors have read and agreed to the published version of the manuscript.

**Funding:** This work was supported by the National Natural Science Foundation of China (Grant No.: 62371242).

**Data Availability Statement:** All relevant data are within the paper.

**Conflicts of Interest:** The authors declare no known competing financial interests or personal relationships that could have appeared to influence the work reported in this paper.

## References

1. Pareek, N.K.; Patidar, V.; Sud, K.K. Image encryption using chaotic logistic map. *Image Vis. Comput.* **2006**, *24*, 926–934.
2. Gao, H.; Zhang, Y.; Liang, S.; Li, D. A new chaotic algorithm for image encryption. *Chaos Solitons Fractals* **2006**, *29*, 393–399.
3. Ma, F.; Wu, L.; Ye, Y.; Zhang, F. A secure multi-party hybrid encryption sharing scheme with a new 2D sine-cosine chaotic system and compressed sensing. *Nonlinear Dyn.* **2024**, *112*, 11523–11546.
4. Yao, P.; Wu, H.; Gao, B.; Tang, J.; Zhang, Q.; Zhang, W.; Yang, J.J.; Qian, H. Fully hardware-implemented memristor convolutional neural network. *Nature* **2020**, *577*, 641–646.
5. Zhang, G.; Shen, Y. Exponential stabilization of memristor-based chaotic neural networks with time-varying delays via intermittent control. *IEEE Trans. Neural Netw. Learn. Syst.* **2014**, *26*, 1431–1441.
6. Xu, Q.; Ding, X.; Chen, B.; Parastesh, F.; Iu, H.H.-C.; Wang, N. A universal configuration framework for mem-element-emulator-based bionic firing circuits. *IEEE Trans. Circuits Syst. I Regul. Pap.* **2024**, *71*, 4120.
7. Xu, Q.; Fang, Y.; Wu, H.; Bao, H.; Wang, N. Firing patterns and fast–slow dynamics in an N-type LAM-based FitzHugh–Nagumo circuit. *Chaos Solitons Fractals* **2024**, *187*, 115376.
8. Feng, W.; Jiang, N.; Zhang, Y.; Jin, J.; Zhao, A.; Liu, S.; Qiu, K. Pulsed-chaos MIMO radar based on a single flat-spectrum and Delta-like autocorrelation optical chaos source. *Opt. Express* **2022**, *30*, 4782–4792.
9. Chen, J.D.; Wu, K.W.; Ho, H.L.; Lee, C.T.; Lin, F.Y. 3-D multi-input multi-output (MIMO) pulsed chaos lidar based on time-division multiplexing. *IEEE J. Sel. Top. Quantum Electron.* **2022**, *28*, 1–9.
10. Sheng, Z.; Li, C.; Gao, Y.; Li, Z.; Chai, L. A switchable chaotic oscillator with multiscale amplitude/frequency control. *Mathematics* **2023**, *11*, 618.
11. Sprott, J.C. A new class of chaotic circuit. *Phys. Lett. A* **2000**, *266*, 19–23.
12. de Sousa Vieira, M.; Lichtenberg, A.J. Controlling chaos using nonlinear feedback with delay. *Phys. Rev. E* **1996**, *54*, 1200.
13. Holmes, P. A nonlinear oscillator with a strange attractor. *Philosophical Transactions of the Royal Society of London. Ser. A Math. Phys. Sci.* **1979**, *292*, 419–448.
14. Thomas, R. Deterministic chaos seen in terms of feedback circuits: Analysis, synthesis, “labyrinth chaos”. *Int. J. Bifurc. Chaos* **1999**, *9*, 1889–1905.
15. Kengne, J.; Njitacke Tabekoueng, Z.; Kamdoum Tamba, V.; Negou, A.N. Periodicity, chaos, and multiple attractors in a memristor-based Shinriki’s circuit. *Chaos Interdiscip. J. Nonlinear Sci.* **2015**, *25*.
16. Sprott, J.C. Some simple chaotic flows. *Phys. Rev. E* **1994**, *50*, R647.

17. Kamdem Kuate, P.D.; Lai, Q.; Fotsin, H. Complex behaviors in a new 4D memristive hyperchaotic system without equilibrium and its microcontroller-based implementation. *Eur. Phys. J. Spec. Top.* **2019**, *228*, 2171–2184.
18. Bao, B.C.; Bao, H.; Wang, N.; Chen, M.; Xu, Q. Hidden extreme multistability in memristive hyperchaotic system. *Chaos Solitons Fractals* **2017**, *94*, 102–111.
19. Zhang, S.; Zheng, J.; Wang, X.; Zeng, Z. A novel no-equilibrium HR neuron model with hidden homogeneous extreme multistability. *Chaos Solitons Fractals* **2021**, *145*, 110761.
20. Njitacke, Z.T.; Doubla, I.S.; Mabekou, S.; Kengne, J. Hidden electrical activity of two neurons connected with an asymmetric electric coupling subject to electromagnetic induction: Coexistence of patterns and its analog implementation. *Chaos Solitons Fractals* **2020**, *137*, 109785.
21. Li, Y.; Liu, J.; Liu, H. A complex-variable disturbed laser with application to hidden multi-scroll attractor generation. *Nonlinear Dyn.* **2024**, *1–19*. <https://doi.org/10.1007/s11071-024-10598-8>
22. Zhang, X.; Li, C.; Lei, T.; Fu, H.; Liu, Z. Offset boosting in a memristive hyperchaotic system. *Phys. Scr.* **2023**, *99*, 015247.
23. Ma, Y.; Mou, J.; Jahanshahi, H.; Alkhateeb, A.F.; Bi, X. Design and DSP implementation of a hyperchaotic map with infinite coexisting attractors and intermittent chaos based on a novel locally active memcapacitor. *Chaos Solitons Fractals* **2023**, *173*, 113708.
24. Ramakrishnan, B.; Tamba, V.K.; Metsebo, J.; Ngatcha, D.T.; Rajagopal, K. Control, synchronisation and antisynchronisation of chaos in two non-identical Josephson junction models via sliding mode control and its FPGA implementation. *Pramana* **2023**, *97*, 46.
25. Karawanich, K.; Chimnoy, J.; Khateb, F.; Marwan, M.; Prommee, P. Image cryptography communication using FPAABased multi-scroll chaotic system. *Nonlinear Dyn.* **2024**, *112*, 4951–4976.
26. Marco, M.D.; Forti, M.; Pancioni, L.; Tesi, A. Drift of invariant manifolds and transient chaos in memristor Chua’s circuit. *Electron. Lett.* **2023**, *59*, e12948.
27. Muni, S.S.; Fatoynibo, H.O.; Ghosh, I. Dynamical effects of electromagnetic flux on chialvo neuron map: Nodal and network behaviors. *Int. J. Bifurc. Chaos* **2022**, *32*, 2230020.
28. Lu, Y.M.; Wang, C.H.; Deng, Q.L.; Xu, C. The dynamics of a memristor-based Rulkov neuron with fractional-order difference. *Chin. Phys. B* **2022**, *31*, 060502.
29. Li, C.; Sprott, J.C. Variable-boostable chaotic flows. *Optik* **2016**, *127*, 10389–10398.
30. Chai, L.; Liu, J.; Chen, G.; Zhang, X.; Li, Y. Amplitude control and chaotic synchronization of a complex-valued laser ring network. *Fractals* **2023**, *31*, 2350091.
31. Li, Y.; Liu, J.; Hao, Z.; Liu, H.; Zhang, X. Multi-scroll hidden hyperchaotic attractor and extreme multistability with offset boosting in a memristor-coupled complex-valued laser network. *Eur. Phys. J. Plus* **2024**, *139*, 1–13.
32. Li, C.; Thio, W.; J.C.; Sprott, J.C.; Iu, H.H.-C.; Xu, Y. Constructing infinitely many attractors in a programmable chaotic circuit. *IEEE Access* **2018**, *6*, 29003–29012.

**Disclaimer/Publisher’s Note:** The statements, opinions and data contained in all publications are solely those of the individual author(s) and contributor(s) and not of MDPI and/or the editor(s). MDPI and/or the editor(s) disclaim responsibility for any injury to people or property resulting from any ideas, methods, instructions or products referred to in the content.